British Journal of Pharmacology (2005) 145, 15–23
www.nature.com/bjp

Pentamidine reduces *hERG* expression to prolong the QT interval

[1]Jason S. Cordes, [1]Zhuoqian Sun, [2]David B. Lloyd, [1]Jenifer A. Bradley, [3]Alan C. Opsahl, [3]Mark W. Tengowski, [1]Xian Chen & *,[1]Jun Zhou

[1]Department of Safety Pharmacology, Pfizer Global Research and Development, Groton/New London Laboratories, MS 8274-1420, Eastern Point Road, Groton, CT 06340, U.S.A.; [2]Department of Genomic and Proteomic Sciences, Pfizer Global Research and Development, Groton/New London Laboratories, MS 8274-1420, Eastern Point Road, Groton, CT 06340, U.S.A. and [3]Department of Pathology, Pfizer Global Research and Development, Groton/New London Laboratories, MS 8274-1420, Eastern Point Road, Groton, CT 06340, U.S.A.

1 Pentamidine, an antiprotozoal agent, has been traditionally known to cause QT prolongation and arrhythmias; however, its ionic mechanism has not been illustrated.

2 In a stable HEK-293 cell line, we observed a concentration-dependent inhibition of the *hERG* current with an IC_{50} of 252 μM.

3 In freshly isolated guinea-pig ventricular myocytes, pentamidine showed no effect on the L-type calcium current at concentrations up to 300 μM, with a slight prolongation of the action potential duration at this concentration.

4 Since the effective concentrations of pentamidine on the *hERG* channel and APD were much higher than clinically relevant exposures ($\sim$1 μM free or lower), we speculated that this drug might not prolong the QT interval through direct inhibition of I_{Kr} channel. We therefore incubated *hERG*-HEK cells in 1 and 10 μM pentamidine-containing media (supplemented with 10% serum) for 48 h, and examined the *hERG* current densities in the vehicle control and pentamidine-treated cells.

5 In all, 36 and 85% reductions of the current densities were caused by 1- and 10-μM pentamidine treatment ($P<0.001$ vs control), respectively. A similar level of reduction of the *hERG* polypeptides and a reduced intensity of the *hERG* protein on the surface membrane in treated cells were observed by Western blot analysis and laser-scanning confocal microscopy, respectively.

6 Taken together, our data imply that chronic administration of pentamidine at clinically relevant exposure reduces the membrane expression of the *hERG* channel, which may most likely be the major mechanism of QT prolongation and *torsade de pointes* reported in man.
British Journal of Pharmacology (2005) **145,** 15–23. doi:10.1038/sj.bjp.0706140
Published online 14 February 2005

Keywords: Pentamidine; QT interval; *torsade de pointes*; potassium channel; human *ether-a-go-go*-related gene

Abbreviations: AP, action potential; APD, action potential duration; *hERG*, human *ether-a-go-go*-related gene; *hERG*-HEK, stable human embryonic kidney (HEK-293) cell line expressing *hERG*; I_{Kr}, rapidly activating delayed rectifier potassium current; TdP, *torsade de pointes*

Introduction

The ability of noncardiac drugs to prolong the QT interval and thereby increase the risk of a potentially fatal cardiac arrhythmia known as *torsade de pointes* (TdP) is of concern (Curtis *et al*., 2003; Morganroth, 2004; Roden, 2004). Most drugs reported to prolong the QT interval clinically are thought to act *via* inhibition of the I_{Kr} channel (Roden, 2004; Tamargo *et al*., 2004). Due to technical challenges in dissecting the I_{Kr} current from overlapping outward currents in the native cardiac myocytes, a mammalian cell line stably expressing human *ether-a-go-go*-related gene (*hERG*) (Zhou *et al*., 1998) has become a widely applied screening tool in industry to test the propensity of a drug to inhibit I_{Kr}. The *hERG* is believed to encode the α-subunit of the human I_{Kr} channel (Sanguinetti *et al*., 1995). Evidence of *hERG* inhibition at clinically relevant concentrations correlates with clinical outcomes for most known QT-prolonging agents (Redfern *et al*., 2003).

*Author for correspondence; E-mail: jun_zhou@groton.pfizer.com
Published online 14 February 2005

Pentamidine-induced QT prolongation and TdP have been reported for almost two decades (Jha, 1983; Wharton *et al*., 1987; Bibler *et al*., 1988); however, no electrophysiological studies on its ionic mechanism are found in the literature thus far. Pentamidine is a diamidine antiprotozoal agent used in the treatment of a number of parasitic diseases, notably *Pneumocystis carinii* pneumonia in AIDS patients. Although it is an effective treatment, the incidence of adverse reactions even at therapeutic doses (4 mg kg^{-1} per day) approaches 50% of patients administered (Tracy & Webster 2001). The most severe of these adverse reactions is cardiotoxicity, which may be manifested through QT prolongation, cardiac arrhythmias (e.g. TdP) and sudden death (Owens, 2004). In this study, we examined the effects of pentamidine on the cardiac ion channels expressed in a human embryonic kidney cell line (HEK-293) and in the guinea-pig ventricular myocytes by using the whole-cell patch-clamp technique. Biochemical and laser-scanning confocal imaging analysis were conducted to support the electrophysiological findings. Our results indicate that, instead of directly blocking the I_{Kr}/*hERG* current,

pentamidine inhibits the membrane expression of the *hERG* channel at clinically relevant concentrations. This may be its major mechanism for causing QT prolongation and cardiac arrhythmias in clinic.

Methods

Isolation of ventricular myocytes

All animal experiments were conducted in accordance with the regulations of the US National Institutes of Health (NIH Publication No. 8523, revised 1996) and European guidelines. Experimental protocols were approved by the Pfizer Institutional Animal Care and Use Committee (ACUP#: 2003-10524-0004). Ventricular myocytes were isolated from male Hartley guinea-pigs. Animals weighing 250–300 g (Charles River Laboratories, Wilmington, MA, U.S.A.) were decapitated following manual restraint and the hearts were quickly removed and placed into Ca^{2+}-free isolation solution. The heart was manually cleared of debris and blood clots, then mounted *via* the aorta to a Langendorff apparatus and perfused retrogradely for 5 min with oxygenated Ca^{2+}-free Isolation Solution (37°C). This was followed by perfusion for 15–20 min with the same solution, but containing collagenase 1 (277 $\mu g\,ml^{-1}$; Sigma) and protease (7.3 $\mu g\,ml^{-1}$; Sigma) and subsequent perfusion with enzyme-free Isolation Solution for 5 min. The ventricles were isolated, placed in Storage Solution and chopped into pieces with scissors. The cell suspension was then filtered through wire mesh and the cells were stored in Storage Solution at room temperature for at least 1 h prior to use. Some experiments were conducted on cells that were stored in the refrigerator overnight and warmed to room temperature before use on the second day.

Patch-clamp recording

hERG-HEK cells (Zhou *et al*., 1998) were licensed from Wisconsin Alumni Research Foundation or generated in house. Minimum essential media (Invitrogen, Carlsbad, CA, U.S.A.) supplemented with 0.1 mM nonessential amino acid (Invitrogen), 1.0 mM sodium pyruvate, 10% fetal bovine serum and 0.05% geneticin (G418, Invitrogen) were used to culture them. On the day of the experiment, cells were dissociated from the flasks using 0.05% trypsin-EDTA and stored at room temperature in M199 medium (Hank's salt).

Aliquots of *hERG*-HEK cells or ventricular myocytes were allowed to settle to the glass bottom of a recording chamber on the inverted microscope (Olympus IX51, Japan) and continually superfused with Tyrode's solution at a rate of 1.0 ml min^{-1}. The *hERG* currents and action potentials (APs) were measured at 35 ± 1°C (maintained by TC344B Temperature Controller, Warner Instruments, CT, U.S.A.) and I_{Ca} was recorded at room temperature. Whole-cell configuration was formed with a glass pipette having a tip resistance of 1–4 MΩ when filled with pipette solution. An EPC-9 (HEKA Elektronik, Germany) or a MultiClamp 700A (Axon Instruments, CA, U.S.A.) patch-clamp amplifier was used with Pulse + PulseFit (v8.40) or pClamp (v8.2) software, respectively. Cell capacitance and series resistance were routinely compensated to reduce the voltage error (limited to 5 mV in an experiment). A giga-ohm (GΩ) seal resistance was achieved in all experiments. Following cell membrane rupture, at least 5 min were allowed for cell dialysis before any recording. For potency tests, 3–5 min of stable recording was performed prior to the application of compound to serve as a baseline control. Cells exhibiting significant rundown of the current (e.g. $\geqslant 2\%\ min^{-1}$) over the baseline period were discarded. In the presence of the drug, a steady-state response was achieved before a subsequent concentration was applied.

The *hERG* currents were elicited by 1-s voltage pulses to + 20 mV from a holding potential of −80 mV, followed by a repolarizing ramp back to −80 mV at a rate of 0.5 V s^{-1} (Volberg *et al*., 2002). To evaluate the drug effect, test pulses were delivered to the cell at 0.25 Hz. At the end of each experiment, 10-μM dofetilide was applied to block any remaining *hERG* current. The dofetilide-insensitive current, which reflects the possible leakage and endogenous currents, was then subtracted from the experimental data. The L-type calcium current (I_{Ca}) was recorded from myocytes under the whole-cell configuration. Cells were held at −70 mV and I_{Ca} was elicited by a 250-ms depolarization to 10 mV following a 200-ms prepulse at −50 mV to inactivate the T-type current, if present.

Nifedipine (10 μM) was applied to the cells at the end of the experiment to evaluate the possible leak current. To quantify the blockade of a compound, a linear fit was applied to the stabilized control data and extrapolated over the period of test compound application to predict the current 'rundown'. Percent block was then computed from the predicted current obtained from the linear extrapolation ($I_{Control}$) to the steady-state response in the presence of the compound (I_{Drug}). APs were recorded from freshly isolated myocytes using the perforated-patch technique with amphotericin B (120 $\mu g\,ml^{-1}$) included in the pipette solution. Cells were injected with a suprathreshold current at 0.5 Hz for 5 ms under current-clamp mode to elicit the APs.

Cell culture and Western blot analysis

hERG-HEK were cultured in Dulbecco's minimal essential media (DMEM, Invitrogen) containing 10% fetal bovine serum (Invitrogen) and 700 $\mu g\,ml^{-1}$ gentamicin (Invitrogen). Cells were seeded at 300,000 cells per well in a six-well plate and incubated overnight at 37°C with 5% CO_2. Media was replaced with 4 ml of fresh media containing 0, 1, 3 and 10 μM pentamidine (in triplicate) and cells were incubated for 48 h (with a media change after 24 h). Cells were harvested in physiologically buffered saline (PBS) and the whole-cell lysates prepared in lysis buffer (50 mM Tris–HCl (pH 8.0), 150 mM NaCl, 24 mM $MgCl_2$, 0.5 mM Na-*o*-vanidate, 10% glycerol, 0.1% NP-40). Protein concentrations were estimated using the Bradford assay. In all, 10 μg of protein per sample was electrophoresed on a 4–12% bis-acrylamide NuPage gel (Invitrogen) in 1 × MES buffer, and transferred to nitrocellulose using a semi-dry transfer cell (BioRad). Membranes were probed with a rabbit antibody against *hERG* (Alomone Labs, APC-062 rabbit anti-human *hERG*), and developed using Super Signal West Pico chemiluminescent substrate (Pierce). To normalize the *hERG* expression levels to a reference protein, membranes were stripped in Restore™ Western blot stripping buffer (Pierce) and re-probed with an antibody against GAPDH (Santa Cruz). Blots were analyzed and

quantitated on a GeneGnome chemiluminescence detection system (Syngene).

Laser-scanning confocal microscopy

hERG-HEK cells were grown to 50–80% confluence using a phenol red-free medium to reduce background fluorescence. The cells were grown at 37°C in 5% CO_2 on round #1.5 coverslips in 16-well culture plates. Live cells were observed prior to further processing using phase-contrast illumination on an inverted microscope to assure adhesion. Cells were washed with PBS and fixed with 3.7% formalin in PBS for 10 min at 37°C. Fixed cells were permeabilized with 0.2% Triton X-100 in PBS for 10 min at 37°C. Nonspecific binding was reduced with an incubation in PBS containing 0.2% Triton X-100 and 1% BSA for 20 min at 37°C. A primary rabbit polyclonal antibody (Alomone Labs, APC-062 rabbit anti-human *hERG*) was diluted 1 : 200 in PBS containing 0.2% Triton X-100 and 1% BSA, and the cells were exposed for 60 min at 37°C. A dye-coupled secondary conjugate (Molecular Probes, Alexa568 goat-anti rabbit IgG) was diluted 1 : 200 in PBS containing 0.2% Triton X-100 and 1% BSA for 60 min at 37°C, completing the indirect immunocytochemistry. DNA was labeled with TOTO-3 (1 μM final) in the last 10 min of the secondary antibody incubation. The cells were washed with copious amounts of PBS between steps. The coverslips were blotted of excess PBS and mounted to frosted glass microscope slides containing an anti-fade medium (Vecta-Shield), sealed with nail polish, and stored flat in the dark at 4°C prior to confocal microscopy. Digital images were collected sequentially using a Leica DMRE upright microscope and Leica SP laser-scanning confocal scan head using appropriate lasers and spectrophotometer setting matched to the above fluorochromes. Images were captured using a $\times 63$ oil objective (NA 1.3) with a zoom factor of 3. DNA and *hERG* fluorescence intensities were quantitated using the line profile measurement tool in ImagePro Plus 5.0. Intensity values were exported to Microsoft Excel and graphically presented. A photomicrograph plate (Figure 5) was created from the confocal TIFF files using Adobe PhotoShop 6.0.

Chemicals and solutions

For isolation of the myocytes, the calcium-free Isolation Solution was composed of (in mM): NaCl, 137; KCl, 5.4; Hepes, 10; $MgCl_2 \cdot 6H_2O$, 1; $NH_2PO_4 \cdot H_2O$, 0.33; D-glucose, 10 (pH 7.4) with NaOH. The Storage Solution contained (in mM): glutamic acid, 50; EGTA, 0.5; glucose, 10; Hepes, 10; KCl, 40; KH_2PO_4, 20; KOH, 70; $MgCl_2 \cdot 6H_2O$, 3; Taurine, 20 (pH 7.4) with NaOH. For the recording of the calcium currents, the bath solution was composed of (in mM): Tris, 137; $CaCl_2$, 1.8; $MgCl_2 \cdot 6H_2O$, 1; glucose, 5; CsCl, 20 (pH 7.4) with CsOH. The internal pipette solution was composed of (in mM): CsCl, 125; MgATP, 5; Hepes, 10; EGTA, 15; TEA-Cl, 20 (pH 7.2) with CsOH. The bath solution used to record the APs was the Isolation Solution with the addition of $CaCl_2$, 1.8 (pH 7.4) with NaOH, and the pipette solution contained (in mM): KCl, 130; MgATP, 5; $MgCl_2$, 1; Hepes, 10; EGTA, 5; Amphotericin B, 120 $\mu g\,ml^{-1}$ (pH 7.2) with KOH. For the *hERG* current recording from the *hERG*-HEK cells, the bath (Tyrode's) solution was composed of (in mM): NaCl, 137; KCl, 4; $CaCl_2$, 1.8; $MgCl_2$, 1; glucose, 10; Hepes, 10 (pH 7.4) with NaOH. The pipette solution contained (in mM): KCl, 130; MgATP, 5; $MgCl_2$, 1; Hepes, 10; EGTA, 5 (pH 7.2) with KOH.

All chemicals were purchased from Sigma-Aldrich (St Louis, MO, U.S.A.). Pentamidine isothionate (Sigma) was dissolved in dimethyl sulfoxide (DMSO) at 100 mM as a stock solution, and then added into the bath solution to a desired test concentration. DMSO concentration in the drug-containing solutions was limited to 0.3%, at which DMSO does not have any noticeable effect on the ionic currents of interest.

Data analysis

Data were expressed as mean ± s.e. A paired Student's *t*-test was used to evaluate the significance of the difference between the means before and after application of drugs. Analysis of variance (ANOVA) was applied to evaluate the multiple group data. A $P<0.05$ was accepted as a statistically significant level. Curve fittings and graphing were performed using Origin v7.0 software (OriginLab Cooperation, Northampton, MA, U.S.A.).

Results

Acute effect of pentamidine on the hERG *current*

The direct effect of pentamidine on the *hERG* current was first examined in the stable *hERG*-HEK cells. As illustrated in Figure 1a, pentamidine inhibited the *hERG* current in a concentration-dependent manner when tested at a range of 10–300 μM. The onset of the block appeared relatively slow, for at least 4–5 min were required to reach a steady state. Averaged concentration–response data from 4–5 experiments were fitted with a Hill equation, which gave an IC_{50} of 252 μM (Figure 1b) with a Hill coefficient of 1.2, indicating a single binding site on the *hERG* channel for this drug.

The blocking mechanism of pentamidine on the *hERG* channel was further explored (Figures 2 and 3). Voltage-dependent *hERG* currents were elicited by a series of 1-s depolarization pulses ranging from −70 to +40 mV from the holding potential of −80 mV. A repolarization at −70 mV was used to elicit the tail current (Figure 2a). Pentamidine was administered at about its IC_{50} concentration and the current values before and after drug exposure were collected. The current–voltage (*I–V*) relationship was constituted in Figure 2b by plotting the developing current amplitudes at the end of depolarization pulses. To evaluate the voltage dependence of the steady-state activation, tail currents were measured, normalized and plotted against the prepulse voltages (Figure 2c). Data were fitted with a Boltzmann function: $I \times I_{max}^{-1} = 1\{1 + \exp[(V_{1/2} - V_m)k^{-1}]\}^{-1}$, where I represents the tail current, V_m is the test membrane potential, $V_{1/2}$ is the half-maximal activation voltage, and k is the slope factor representing the steepness of the voltage dependence. A slight but statistically significant shift (−4.2 ± 0.8 mV) in the half-activating voltage ($V_{1/2}$) was observed as a result of the drug administration (−36.4 ± 2.1 mV after 250 μM pentamidine vs −32.2 ± 1.7 mV before drug, $n=5$, $P<0.01$). The steepness of the voltage dependence also appeared slightly suppressed (4.7 ± 0.3 mV after drug vs 5.7 ± 0.3 mV control, $P=0.04$). The small change in the voltage dependence reflected a modest voltage-dependent block of pentamidine, which was more

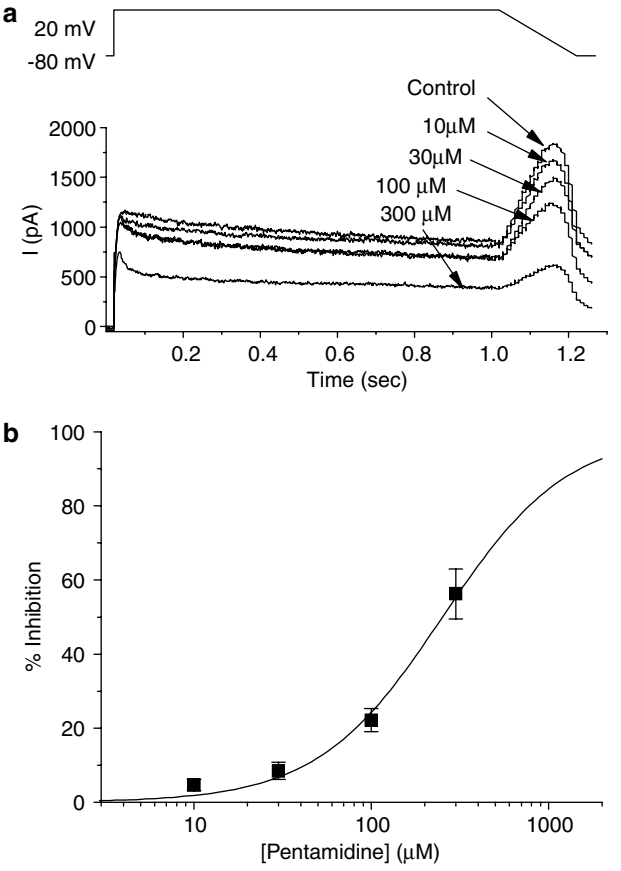

Figure 1 Pentamidine block of the *hERG* current in stable *hERG*-HEK cells. (a) Representative current traces before and after administration of pentamidine at various concentrations. The voltage protocol used to elicit the *hERG* current is shown in the upper panel. (b) Concentration–response curve of the pentamidine effect. Averages of 4–5 experiments were fitted with a Hill equation and an IC_{50} of 252 μM was obtained.

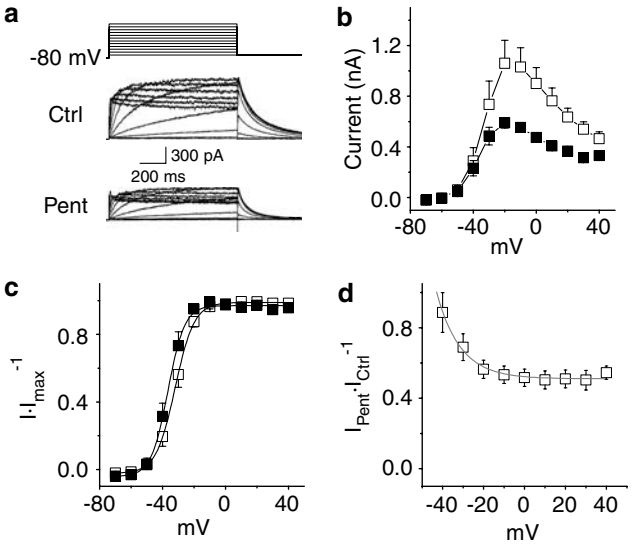

Figure 2 Voltage-dependent blocking of pentamidine on the *hERG* channel. (a) Typical current traces at different voltages in the absence (Ctrl) and presence of 250-μM pentamidine (Pent). Cells were held at −80 mV, depolarized to a series of steps ranging from −70 to +40 mV for 1 s, and followed by a repolarization pulse at −70 mV to elicit the tail current. (b) Current–voltage (*I–V*) relationship of the *hERG* channel. Developing currents measured at the end of each depolarization pulse were summarized from five experiments. Open and closed squares indicate control and 250 μM pentamidine groups, respectively. (c) Effect of pentamidine on the voltage dependence of steady-state activation (square symbols). Averaged data from five experiments were fitted with a Boltzmann function, resulting in a half-activation voltage and a slope factor of −32.0 and 6.0 mV, respectively, for the control (open squares), and −36.6 and 5.3 mV, respectively, for pentamidine (closed squares). (d) Voltage-dependent block by pentamidine was computed from the tail currents in the presence of drug normalized to the control (I_{Pent}−I_{Ctrl}^{-1}). A single exponential function was applied to fit the averaged data from five observations.

evident in the range between −40 and −10 mV (Figure 2d; $I_{Drug} \times I_{Control}^{-1}$ was computed from the tail current). Averages of 11.4, 31.1, 43.6 and 46.7% inhibition of the *hERG* current were observed at −40, −30, −20 and −10 mV, respectively, and there was no further increase at higher potentials. The relationship between the blockade and the membrane potentials can be described by a single-exponential equation: $y = y_0 + A\exp(-V_m s^{-1})$, where s defines the steepness of the voltage dependence and y_0 reflects the maximum block. The fitting on five experiments yielded an s of 16.8±4.2 mV and y_0 of 0.49±0.05 (i.e. ~51% block).

The voltage-dependent blockade of *hERG* by pentamidine and its relatively slow blocking kinetics prompted us to investigate if this drug acted as an open-channel blocker. We therefore superfused the cells with 250 μM pentamidine without stimulation for 5 min after the control currents were stabilized (Figure 3a, open circles). In all, 5 min were shown to be sufficient for the drug to reach its steady-state blockade (Figure 2d, open squares). Since the cells were held at −80 mV, *hERG* channels during the 5-min period stayed at the closed state. A typical open-channel blocker such as E-4031 had been shown previously (Volberg *et al.*, 2002) to have no binding to the closed channel and therefore the first stimulation-elicited current was comparable to the control level. However, in the presence of pentamidine, the first current after the 5-min break was at a similar percentage blocking level when compared to that of the steady-state blockade. No further increase in blocking was observed at consecutive pulses. These data suggest that pentamidine may bind to the closed channel and therefore its blockade does not require the channel to open. However, similar results might also be produced by a super fast open-channel blocker such as cocaine under these testing conditions (Zhang *et al.*, 2001). To address this issue, we investigated the time course of the depolarization-activated *hERG* current in an attempt to identify the development of blocking and, if any, the blocking kinetics. Current traces elicited by a series of test potentials ranging from −70 to +40 mV were compared between those in the presence and absence of 250 μM pentamidine. As shown in Figure 3b, no apparent time-dependent decline of the current by the compound was seen at 0 and 20 mV, potentials at which the *hERG* channel could be fully activated (Figure 2c). Moreover, we used a voltage protocol similar to what was applied for cocaine (Zhang *et al.*, 2001) to see if a fast blocking activity might have developed during very early depolarization. By this protocol, the *hERG* current was rapidly activated by a 5-ms strong depolarization pulse at +100 mV from the holding potential of −80 mV, followed by a 100-ms step to 0 mV. The current elicited at 0 mV was nearly instantaneous and

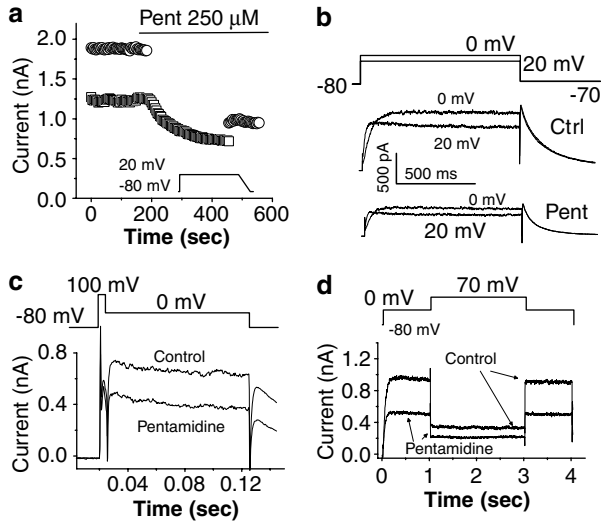

Figure 3 Blocking mechanism of pentamidine. (a) Pentamidine block of *hERG* during continuous stimulation (open squares) and after holding the cell at −80 mV for 5 min (open circles) to keep the channel at closed state. A 5-min period was sufficient for a steady-state block during normal perfusion and stimulation when pentamidine (250 μM) was administered. Currents were elicited by a voltage protocol used for the potency determination (Figure 1) as shown in the inset. Tail current amplitude was measured and plotted. Note that the first stimulation after the 5-min pause elicited a percentage of current comparable to that at the steady-state block level and no further increase of the block was observed following consecutive stimuli. (b) Current traces at 0 and +20 mV in the presence and absence of 250-μM pentamidine. Voltage protocol was shown in the inset. No apparent time-dependent development of blocking was observed in the depolarization-activated currents at both potentials. (c) Pentamidine block does not require channel activation. Using a voltage protocol shown at the top, *hERG* current was rapidly activated from a holding potential of −80 mV by a 5-ms depolarizing step to 100 mV, followed by a step to 0 mV for 100 ms. The first stimulation after 5-min wash-in of 250 μM pentamidine elicited a significantly reduced (~50%) current which was almost in parallel to the control. Similar results were observed in four experiments. (d) Pentamidine block during a strong membrane depolarization. Currents were recorded from a representative cell before and after application of 250-μM pentamidine. Voltage protocol shown in the upper panel included a first depolarization at 0 mV for 1 s, then at +70 mV for 2 s, and finally at 0 mV again for 1 s. Percent block at the end of each step was computed.

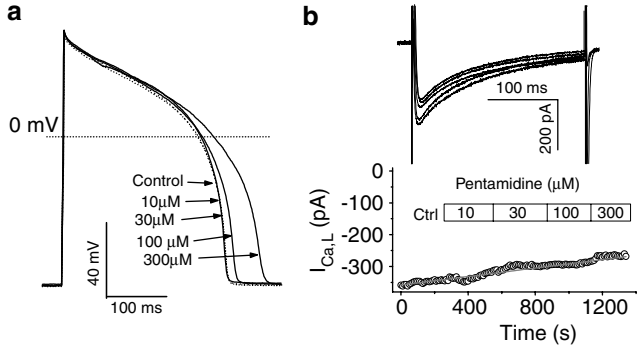

Figure 4 Effects of pentamidine on the APs (a) and L-type calcium channel current (b) in freshly isolated guinea-pig ventricular myocytes. APs were recorded by using perforated-patch technique and elicited by suprathreshold stimulations under current-clamping mode. L-type calcium currents were elicited by a depolarization to +10 mV from a prepulse at −50 mV. Current traces shown in upper panel b were from a representative experiment, and the superimposed recordings, from bottom up, represent control, 10, 30, 100 and 300 μM pentamidine, respectively. In the time course of the peak current amplitude (lower panel b), a linear fit to the control values was extrapolated throughout the experiment, which indicated no noticeable effect of pentamidine at the test concentrations.

constant, which provided a higher resolution for evaluating the blocking kinetics of an ultra-rapid open-channel blocker such as cocaine (Zhang *et al*., 2001). However, as shown in Figure 3c, the first current trace after a 5-min pause during wash-in of 250 μM pentamidine demonstrated a time course similar to that prior to drug application. Taken together, it is highly likely that pentamidine can bind to the closed channel and its block does not require the channel to open.

To determine if the inactivation state was involved in the voltage-dependent blockade, we employed an additional protocol in which a sustained 4-s depolarization from −80 mV was composed of three phases. The first phase was set at 0 mV for 1 s, followed by a 2-s higher depolarization at +70 mV and return to 0 mV. The level of blockade during each phase was measured. As shown in Figure 2f, the current amplitude decreased significantly during the second phase at +70 mV, reflecting the fact that +70 mV favors the channel inactivation. In the presence of 250 μM pentamidine, the *hERG* current blockade measured at the end of the three phases were 40.3±3.2, 31.6±2.0 and 39.9±4.9%, respectively ($n=3$, $P=0.23$). The results suggest that an extensive *hERG* inactivation at +70 mV does not significantly change the avidity of the drug binding.

Effects of pentamidine on I_{Ca} *and AP in guinea-pig ventricular myocytes*

Although I_{Kr} is the most important repolarizing current in the human heart, theoretically any changes that may break the net inward/outward current balance from a normal heart may lead to alterations in the shape and/or duration of the AP. Indeed, some QT prolonging agents have been found to possess multiple channel-blocking activities, which often mitigate or exacerbate the prolongation of APD and QT that would ensue from block of I_{Kr} alone (Redfern *et al*., 2003). To further estimate the possible effects of pentamidine on other ion channels and how these effects may alter the integrated AP, we recorded APs from guinea-pig ventricular myocytes. Perforated patch technology was used in order to obtain a stable AP recording from a single myocyte. Pentamidine was given at 10, 30, 100 and 300 μM. A representative experiment was shown in Figure 4a. No significant effect was seen on the APs at up to 30 μM. At 100 and 300 μM, averages of 9 and 30% prolongation in APD_{90} were induced ($n=3$ at each concentration). No major changes in other parameters of the AP, including the maximal upstroke velocity (V_{max}), resting membrane potential (RMP), and the AP amplitude (APA) were observed.

A direct investigation on the ion channel effect was performed on I_{Ca}, a frequent target of those mixed channel blockers. Freshly isolated myocytes from guinea-pigs were superfused at room temperature with pentamidine-containing solutions at concentrations ranging from 10 to 300 μM. Cells were held at −70 mV, which helped to minimize the rundown of the calcium current. I_{Ca} was elicited by a depolarization to

+10 mV from a prepulse at −50 mV. As shown in Figure 4b, after rundown correction, no significant effect of pentamidine on I_{Ca} was observed at concentrations up to 300 μM. Similar results were observed in two other experiments.

Inhibition of hERG *expression by pentamidine at therapeutic concentrations*

Although an inhibitory effect of pentamidine on the *hERG* current and its ability to prolong the APD had been confirmed, the concentrations at which these changes occurred appeared to be far off the clinically relevant exposures. Peak plasma concentrations (C_{max}) were reported at 612 ng ml^{-1} (1.8 μM total or 0.54 μM protein-unbound) within 60 min of a 4 mg kg^{-1} i.v. injection (Conte *et al*., 1986) or following a single 2-h intravenous infusion of 4 mg kg^{-1} of pentamidine isethionate (Prod Info NebuPent®, 1997). Circulatory concentrations when administered through other routes are even less, often below 50 ng ml^{-1} (<0.15 μM total or 0.045 μM protein-unbound). Therefore, the IC_{50} of pentamidine on the *hERG* current (252 μM) represents at least 467-fold of its protein-free C_{max} following an i.v. injection, which is in direct contrast to what was proposed recently (~30-fold margin) for a typical QT-prolonging agent (Redfern *et al*., 2003). We therefore speculated that pentamidine may not exert its effect on cardiac repolarization directly through I_{Kr} inhibition. To test this hypothesis, we incubated the *hERG*-HEK cells in vehicle- or pentamidine-containing (1 or 10 μM) media at 37°C for 48 h. At 10 μM, we observed that the cell growth was slower and some of the cells were floating on the surface of the media, indicating this concentration might be close to its cytotoxicity level. The *hERG* current densities were examined by using the whole-cell patch-clamp technique in normal Tyrode's solution. Peak tail currents, elicited by the same voltage protocol as used in evaluating the potency, were measured and are summarized in Figure 5a. As compared with the vehicle-treated control, 36 and 85% reductions of the *hERG* current densities were observed in the cells treated with 1 and 10 μM pentamidine, respectively (n = 23–32, P < 0.001 by ANOVA).

Pentamidine-treated *hERG*-HEK cells were also examined for the expression of the *hERG* polypeptide by using the Western blot analysis. Whole-cell lysates were prepared and electrophoresed on a 4–12% bis-acrylamide gel, and subsequently transferred to nitrocellulose. The membrane was probed with a *hERG* antibody, stripped and reprobed with an antibody against GAPDH. The *hERG* band (~155 kb) densities were measured and normalized against the corresponding GAPDH levels (Figure 5b). The results indicated 44% (P < 0.05) and 81% (P < 0.001) reductions of the *hERG* polypeptide in cells treated with 3 and 10 μM pentamidine, respectively.

In an attempt to localize the *hERG* polypeptide in the *hERG*-HEK cells, laser-scanning confocal imaging analysis was performed. Images of representative cell fields treated with either vehicle control or 1 μM pentamidine are shown in Figure 6. The *hERG* channel and nuclear staining are represented as red and blue fluorescence, respectively. The optical sections of control *hERG*-HEK cells (Figure 6a) displayed a high intensity of *hERG* channel staining in the region of the cellular membrane with little *hERG*-specific fluorescence in the cytoplasm. In contrast, *hERG*-HEK cells in the presence of 1-μM pentamidine appeared to manifest more diffused *hERG* fluorescence across the cytoplasm (Figure 6b), unlike the clear rim-like distribution in the surface membrane commonly observed in control cells. Line profiles measuring fluorescence intensity for DNA and *hERG* staining were

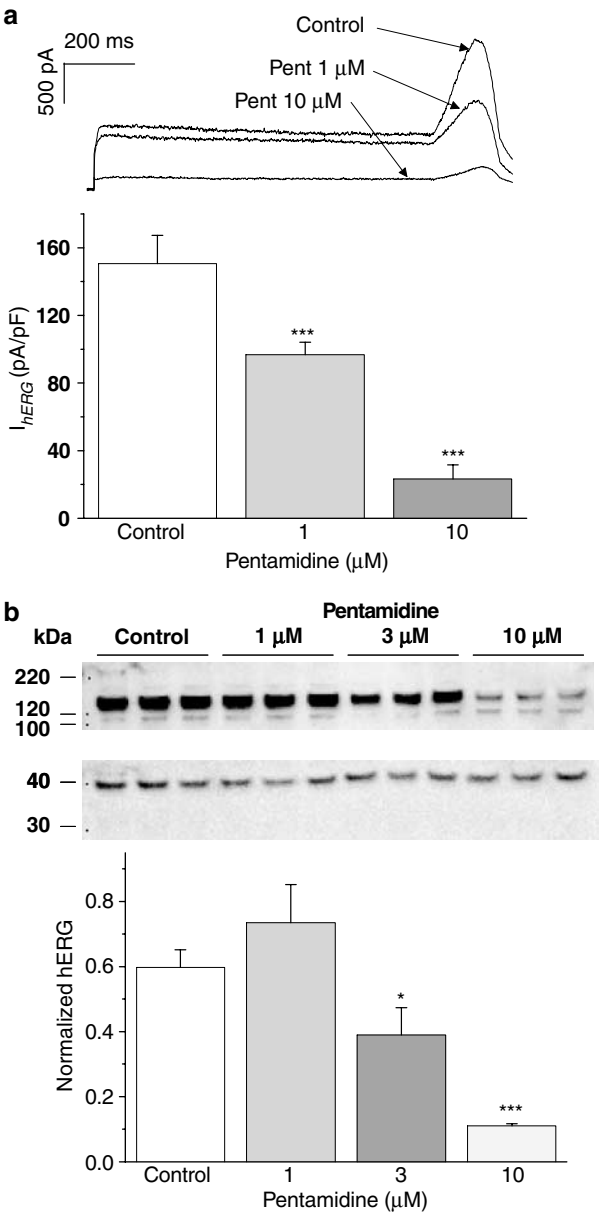

Figure 5 Pentamidine inhibits the surface membrane expression of the *hERG* channel. (a) Decreased *hERG* current as a result of pentamidine treatment. The *hERG*-HEK cells were incubated for 48 h in culture media containing 1- or 10-μM pentamidine or its vehicle before the patch-clamp measurement. Current traces were elicited by the same voltage protocol as shown in Figure 1. Current densities were summarized from the three groups (n = 26, 32 and 23 for control, 1 and 10 μM pentamidine, respectively). ***P < 0.001. (b) Decrease of *hERG* polypeptide in the pentamidine-treated cells detected by Western blot analysis. Whole-cell lysates were prepared and electrophoresed on a 4–12% bis-acrylamide gel, and subsequently transferred to nitrocellulose. The membrane was probed with a *hERG* antibody (upper gel), stripped and reprobed with an antibody against GAPDH (lower gel). The *hERG* band (~155 kb, upper gel) densities were measured, normalized against the corresponding GAPDH levels, and are summarized in lower panel b.

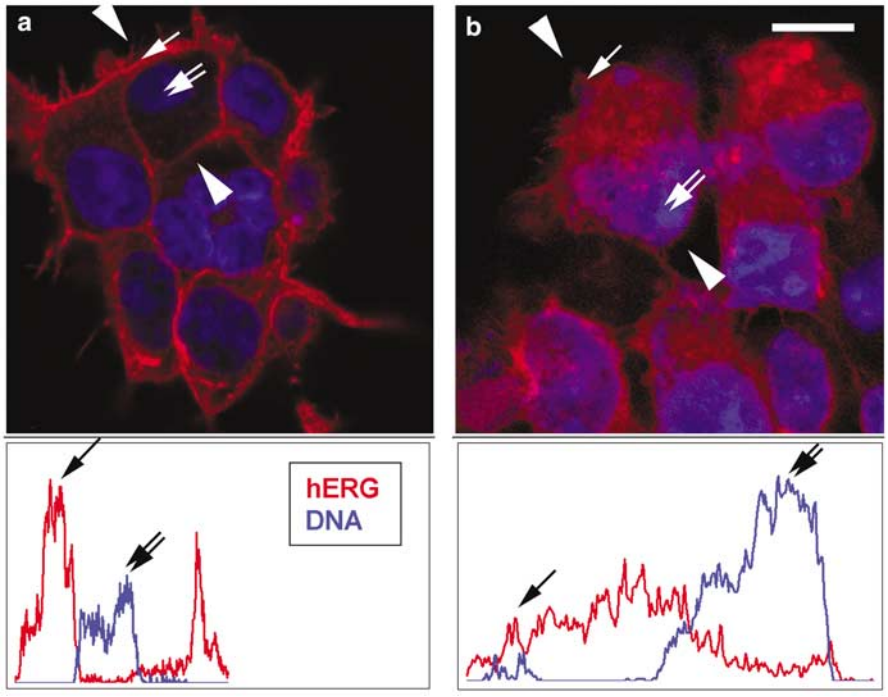

Figure 6 Pentamidine exposure to *hERG*-HEK cells reduces surface membrane expression of the *hERG* channel. Laser-scanning confocal microscopy optical sections of control *hERG*-HEK cells (a) and cells in the presence of 1 μM pentamidine (b). The *hERG* polypeptide was recognized using an indirect fluorescence method and pseudocolored red; DNA was labeled with an intercalating dye and pseudocolored blue. Arrowheads in (a) and (b) are the bounds of the line profile for fluorescence intensities. The line begins with the left arrowhead and stops at the right arrowhead. Fluorescence intensities for both *hERG* polypeptide (single arrow) and DNA (double arrow) are graphically represented on the histogram plot. A single arrow marks a region of cell membrane, with a double arrow marking the nucleus. Changes in both *hERG* and DNA fluorescence signals can be appreciated along the line profiles. Scale bar = 10 μm.

generated across single control and 1-μM pentamidine-treated cells (Figure 6, arrowheads). The intensity graphs support the visual observation that *hERG* staining localizes to the cell membrane in control cells but is distributed diffusely across cells in the presence of 1-μM pentamidine.

Discussion

Pentamidine has been an effective therapy for decades against a number of pathogenic protozoa, especially *P. carinii* in patients who cannot tolerate trimethoprim-sulfamethoxazole (Tracy & Webster, 2001). However, there are at least 14 reports of QT interval prolongation, severe ventricular arrhythmias including *TdP* and/or sudden cardiac death by this drug (Girgis *et al*., 1997; Owens, 2004). As a result, the European Agency for the Evaluation of Medicinal Products (EMEA) and the U.S. Food and Drug Administration (FDA) routinely list pentamidine in the warning labels to discourage its concomitant use with other drugs that have QT-prolonging potential. Interestingly, there are no reports found in the literature about its effect on *hERG* or I_{Kr}, the most important contributor to drug-induced QT prolongation and cardiac arrhythmias. In this study, we first investigated the electrophysiological effect of this well-known QT-prolonging agent. Our data indicate that this compound could indeed block the *hERG* channel, with an IC_{50} of 252 μM. As pentamidine and the antiarrhythmic procainamide share a similar pharmacophore (De Ponti *et al*., 2000), we examined the blocking mechanism of pentamidine in an attempt to compare it with that reported previously for procainamide (Ridley *et al*., 2003). Similar to procainamide, pentamidine also exerted a voltage-dependent block of the *hERG* channel, especially in the range of relatively low depolarization voltages ($-40 \sim -10$ mV). However, in contrast to procainamide's open-channel blocking characteristic, pentamidine blockade does not require the channel to open, indicating that it can access and bind to the *hERG* channel when it is closed. In addition, procainamide was shown to have a significant decrease in the extent of *hERG* blocking when the channel underwent an extensive inactivation, implying that conformational changes of the channel due to inactivation reduced the avidity of the drug binding. In contrast, only a negligible inactivation-induced reduction of block was observed in the case of pentamidine, which is unlikely to contribute to its voltage-dependent blockade because the voltage dependence was mainly seen at low potentials. Pentamidine is expected to exist as a positively charged molecule at physiological pH, as it contains two basic amidine functional groups with a calculated pK_a of 12.50 and 11.89, respectively (ACD/Labs 6.0, Toronto, Canada). It is therefore highly possible that further depolarization enhances the accessibility and/or affinity of the drug to the *hERG* channel through electrostatic interaction.

From this study, it appears that the effective concentrations of pentamidine to directly inhibit the *hERG* current are far above clinically relevant exposures. The IC_{50} of pentamidine (252 μM) represents at least 467-fold its unbound C_{max} following an i.v. injection (Conte *et al*., 1986) or 5600-fold

unbound C_{max} through other routes of administration (DRUGDEX® – Drug Evaluations, Thomson MicroMedex Database). Further studies on the AP in guinea-pig ventricular myocytes demonstrated that pentamidine prolonged the APD at a similar concentration range, implying that the inhibition of I_{Kr} is the major underlying mechanism of APD prolongation. It also suggests a low probability that pentamidine-induced QT prolongation clinically is due to the drug's interactions with other ion channels. To our surprise, a 48-h incubation of pentamidine at much lower concentrations resulted in a significant reduction in the *hERG* current density detected by patch-clamp experiments in single *hERG*-HEK cells. This effect correlated with the reduction in the surface membrane expression of the *hERG* polypeptide as confirmed in both Western blot analysis and laser-scanning confocal microscopy studies. Although we are uncertain about the exact unbound drug concentrations in these experiments when 10% fetal bovine serum was present in the culture media (70% protein binding fraction in serum), we still expect that concentrations as low as 1 μM (total) reside in the clinically relevant range, especially when the drug is multiple-dosed through intravenous routes (a total of 612 ng ml^{-1} or 1.8 μM concentration was achieved within 60 min of a 4 mg kg^{-1} i.v. injection) (Conte *et al*., 1986). Interestingly, the majority of the TdP cases were reported in patients during the prolonged administration of pentamidine instead of immediately following i.v. injection (Wharton *et al*., 1987; Bibler *et al*., 1988; Cortese *et al*., 1992; Eisenhauer *et al*., 1994; Otsuka *et al*., 1997; Kroll & Gettes, 2002). This seems to support the notion that pentamidine inhibits the expression of *hERG*/I_{Kr}, leading to QT prolongation and arrhythmia. The concentration-dependent suppression of the expression level of the *hERG* channel by pentamidine observed in this study seems to also indicate a much milder effect at the nM level, which occurs when other routes of administration are used. Indeed, no major QT prolongation and cardiac arrhythmia have been reported in patients treated with inhaled pentamidine when exposures are often below 50 ng ml^{-1} or 0.15 μM total, 0.045 μM protein-unbound (Thalhammer *et al*., 1993; Cardoso *et al*., 1997).

The pharmacological effect of pentamidine on the membrane expression of *hERG* may result from inhibition of the channel synthesis and/or trafficking, increased turnover of the membrane protein, or both. The drug is known for its ability to inhibit DNA and protein synthesis in parasites (Dykstra & Tidwell, 1991; Bailly *et al*., 1994), but it is unclear at this stage if a similar mechanism exists in *hERG* protein production at relevant concentrations. The *hERG* channel proteins are synthesized in the endoplasmic reticulum (ER) before being transported to the cell surface *via* the Golgi apparatus. Two steps of glycosylation take place in the ER and Golgi after *hERG* is synthesized. Misfolded and incompletely assembled proteins are retained and degraded in the ER by its quality control mechanism including chaperone-induced correction and proteasomal degradation. Any impairment in the trafficking machinery would lead to a suppression of the membrane protein expression, which has often been associated with *hERG* mutations (Thomas *et al*., 2003). Pharmacologically, arsenic trioxide (As_2O_3) was reported very recently (Ficker *et al*., 2004) as the first example to inhibit the *hERG*-chaperone interaction and therefore reduce the trafficking of *hERG* channels to the cell surface, leading to QT prolongation and TdP in clinic. The manifestation of the pharmacological effect of pentamidine appears very similar to that of arsenic, but whether this drug inhibits the trafficking procedures remains to be further explored. We are currently investigating the various cytoplasmic compartments (e.g. ER- and Golgi-specific) for the location of *hERG* polypeptide in pentamidine-treated cells and the effect on *hERG*-chaperone interaction. These data should help explain the chronology of *hERG* polypeptide expression and dysfunction introduced by the presence of pentamidine in this cell culture system. Interestingly, during the review of this manuscript, *hERG* trafficking blocked by pentamidine was reported by another research group (Kuryshev *et al*., 2005). Our findings are therefore consistent with their study results.

While our work focused on the *hERG* channel, the possibility of pentamidine affecting other ion channels chronically cannot be excluded. Nonetheless, the importance of the *hERG*/I_{Kr} channel in cardiac repolarization and the good correlation between the clinical outcomes and our findings strongly support the notion that pentamidine prolongs the QT interval mainly through inhibition of the *hERG* expression. The findings of this study may have a significant implication in further defining the preclinical QT assessment strategy that is currently focusing on investigations of the acute effects of pharmaceuticals. Examination of the effect on ion channel expression should be considered when compounds have weak or no *hERG* activity, but demonstrate QT prolongation in chronically dosed animals. Our study results provide another example that acquired long-QT syndrome can be caused by pharmaceuticals suppressing the *hERG* channel expression instead of direct blockade of the channel.

We thank Dr Phillip M. Bartholomew for his support during the study and critical review of the manuscript.

References

BAILLY, C., DONKOR, I.O., GENTLE, D., THORNALLEY, M. & WARING, M.J. (1994). Sequence-selective binding to DNA of *cis*- and *trans*-butamidine analogues of the anti-*Pneumocystis carinii* pneumonia drug pentamidine. *Mol. Pharmacol.,* **46,** 313–322.

BIBLER, M.R., CHOU, T.C., TOLTZIS, R.J. & WADE, P.A. (1988). Recurrent ventricular tachycardia due to pentamidine-induced cardiotoxicity. *Chest,* **94,** 1303–1306.

CARDOSO, J.S., MOTA-MIRANDA, A., CONDE, C., MOURA, B., ROCHA-GONCALVES, F. & LECOUR, H. (1997). Inhalatory pentamidine therapy and the duration of the QT interval in HIV-infected patients. *Int. J. Cardiol.,* **59,** 285–289.

CONTE JR, J.E., UPTON, R.A., PHELPS, R.T., WOFSY, C.B., ZURLINDEN, E. & LIN, E.T. (1986). Use of a specific and sensitive assay to determine pentamidine pharmacokinetics in patients with AIDS. *J. Infect. Dis.,* **154,** 923–929.

CORTESE, L.M., GASSER JR, R.A., BJORNSON, D.C., DACEY, M.J. & OSTER, C.N. (1992). Prolonged recurrence of pentamidine-induced torsades de pointes. *Ann. Pharmacother.,* **26,** 1365–1369.

CURTIS, L.H., OSTBYE, T., SENDERSKY, V., HUTCHISON, S., ALLEN LAPOINTE, N.M., AL-KHATIB, S.M., USDIN YASUDA, S., DANS, P.E., WRIGHT, A., CALIFF, R.M., WOOSLEY, R.L. & SCHULMAN, K.A. (2003). Prescription of QT-prolonging drugs in a cohort of about 5 million outpatients. *Am. J. Med.,* **114,** 135–141.

DE PONTI, F., POLUZZI, E. & MONTANARO, N. (2000). QT-interval prolongation by non-cardiac drugs: lessons to be learned from recent experience. *Eur. J. Clin. Pharmacol.,* **56,** 1–18.

DYKSTRA, C.C. & TIDWELL, R.R. (1991). Inhibition of topoisomerases from *Pneumocystis carinii* by aromatic dicationic molecules. *J. Protozool.,* **38,** 78S–81S.

EISENHAUER, M.D., ELIASSON, A.H., TAYLOR, A.J., COYNE JR, P.E. & WORTHAM, D.C. (1994). Incidence of cardiac arrhythmias during intravenous pentamidine therapy in HIV-infected patients. *Chest,* **105,** 389–395.

FICKER, E., KURYSHEV, Y.A., DENNIS, A.T., OBEJERO-PAZ, C., WANG, L., HAWRYLUK, P., WIBLE, B.A. & BROWN, A.M. (2004). Mechanisms of arsenic-induced prolongation of cardiac repolarization. *Mol. Pharmacol.,* **66,** 33–44.

GIRGIS, I., GUALBERTI, J., LANGAN, L., MALEK, S., MUSTACIUOLO, V., COSTANTINO, T. & MCGINN, T.G. (1997). A prospective study of the effect of I.V. pentamidine therapy on ventricular arrhythmias and QTc prolongation in HIV-infected patients. *Chest,* **112,** 646–653.

JHA, T.K. (1983). Evaluation of diamidine compound (pentamidine isethionate) in the treatment resistant cases of kala-azar occurring in North Bihar, India. *Trans. R. Soc. Trop. Med. Hyg.,* **77,** 167–170.

KROLL, C.R. & GETTES, L.S. (2002). T wave alternans and torsades de pointes after the use of intravenous pentamidine. *J. Cardiovasc. Electrophysiol.,* **13,** 936–938.

KURYSHEV, Y.A., FICKER, E., WANG, L., HAWRYLUK, P., DENNIS, A.T., WIBLE, B.A., BROWN, A.M., KANG, J., CHEN, X.L., SAWAMURA, K., REYNOLDS, W. & RAMPE, D. (2005). Pentamidine-induced long QT syndrome and block of HERG Trafficking. *J. Pharmacol. Exp. Ther.,* **312,** 316–323.

MORGANROTH, J. (2004). A definitive or thorough phase 1 QT ECG trial as a requirement for drug safety assessment. *J. Electrocardiol.,* **37,** 25–29.

OTSUKA, M., KANAMORI, H., SASAKI, S., TAGUCHI, J., HARANO, H., OGAWA, K., MATSUZAKI, M., MOHRI, H., OKUBO, T., SUMITA, S. & OCHIAI, H. (1997). Torsades de pointes complicating pentamidine therapy of *Pneumocystis carinii* pneumonia in acute myelogenous leukemia. *Intern. Med.,* **36,** 705–708.

OWENS JR, R.C. (2004). QT prolongation with antimicrobial agents: understanding the significance. *Drugs,* **64,** 1091–1124.

REDFERN, W.S., CARLSSON, L., DAVIS, A.S., LYNCH, W.G., MACKENZIE, I., PALETHORPE, S., SIEGL, P.K., STRANG, I., SULLIVAN, A.T., WALLIS, R., CAMM, A.J. & HAMMOND, T.G. (2003). Relationships between preclinical cardiac electrophysiology, clinical QT interval prolongation and torsade de pointes for a broad range of drugs: evidence for a provisional safety margin in drug development. *Cardiovasc. Res.,* **58,** 32–45.

RIDLEY, J.M., MILNES, J.T., BENEST, A.V., MASTERS, J.D., WITCHEL, H.J. & HANCOX, J.C. (2003). Characterisation of recombinant HERG K+ channel blockade by the Class Ia antiarrhythmic drug procainamide. *Biochem. Biophys. Res. Commun.,* **306,** 388–393.

RODEN, D.M. (2004). Drug-induced prolongation of the QT interval. *N. Engl. J. Med.,* **350,** 1013–1022.

SANGUINETTI, M.C., JIANG, C., CURRAN, M.E. & KEATING, M.T. (1995). A mechanistic link between an inherited and an acquired cardiac arrhythmia: HERG encodes the I_{Kr} potassium channel. *Cell,* **81,** 299–307.

TAMARGO, J., CABALLERO, R., GOMEZ, R., VALENZUELA, C. & DELPON, E. (2004). Pharmacology of cardiac potassium channels. *Cardiovasc. Res.,* **62,** 9–33.

THALHAMMER, C., BOGNER, J.R. & LOHMOLLER, G. (1993). Chronic pentamidine aerosol prophylaxis does not induce QT prolongation. *Clin. Investig.,* **71,** 319–322.

THOMAS, D., KIEHN, J., KATUS, H.A. & KARLE, C.A. (2003). Defective protein trafficking in hERG-associated hereditary long QT syndrome (LQT2): molecular mechanisms and restoration of intracellular protein processing. *Cardiovasc. Res.,* **60,** 235–241.

TRACY, J. & WEBSTER, L. (2001). Drugs used in the chemotherapy of protozoal infections. In: *Goodman & Gilman's The Pharmacological Basis of Therapeutics,* ed. Hardman, J. & Limbird, L. pp. 1097–1120. New York: McGraw-Hill Medical Publishing Division.

VOLBERG, W.A., KOCI, B.J., SU, W., LIN, J. & ZHOU, J. (2002). Blockade of human cardiac potassium channel human *ether-a-go-go*-related gene (HERG) by macrolide antibiotics. *J. Pharmacol. Exp. Ther.,* **302,** 320–327.

WHARTON, J.M., DEMOPULOS, P.A. & GOLDSCHLAGER, N. (1987). *Torsade de pointes* during administration of pentamidine isethionate. *Am. J. Med.,* **83,** 571–576.

ZHANG, S., RAJAMANI, S., CHEN, Y., GONG, Q., RONG, Y., ZHOU, Z., RUOHO, A. & JANUARY, C.T. (2001). Cocaine blocks HERG, but not KvLQT1+minK, potassium channels. *Mol. Pharmacol.,* **59,** 1069–1076.

ZHOU, Z., GONG, Q., YE, B., FAN, Z., MAKIELSKI, J.C., ROBERTSON, G.A. & JANUARY, C.T. (1998). Properties of HERG channels stably expressed in HEK 293 cells studied at physiological temperature. *Biophys. J.,* **74,** 230–241.

(Received September 13, 2004
Revised October 25, 2004
Accepted October 27, 2004)